JOC The Journal of Organic Chemistry
Article
pubs.acs.org/joc

Refined Transition-State Models for Proline-Catalyzed Asymmetric Michael Reactions under Basic and Base-Free Conditions

Akhilesh K. Sharma and Raghavan B. Sunoj*

Department of Chemistry, Indian Institute of Technology Bombay, Powai, Mumbai 400076, India

S Supporting Information

ABSTRACT: The stereocontrolling transition state (TS) models for C−C bond formation relying on hydrogen bonding have generally been successful in proline-catalyzed aldol, Mannich, *α*-amination, and *α*-aminoxylation reactions. However, the suitability of the hydrogen-bonding model in protic and aprotic conditions as well as under basic and base-free conditions has not been well established for Michael reactions. Through a comprehensive density functional theory investigation, we herein analyze different TS models for the stereocontrolling C−C bond formation, both in the presence and absence of a base in an aprotic solvent (THF). A refined stereocontrolling TS for the Michael reaction between cyclohexanone and nitrostyrene is proposed. The new TS devoid of hydrogen bonding between the nitro group of nitrostyrene and carboxylic acid of proline, under base-free conditions, is found to be more preferred over the conventional hydrogen-bonding model besides being able to reproduce the experimentally observed stereochemical outcome. A DBU-bound TS is identified as more suitable for rationalizing the origin of asymmetric induction under basic reaction conditions. In both cases, the most preferred approach of nitrostyrene is identified as occurring from the face *anti* to the carboxylic acid of proline−enamine. The predicted enantio- and diastereoselectivities are in very good agreement with the experimental observations.

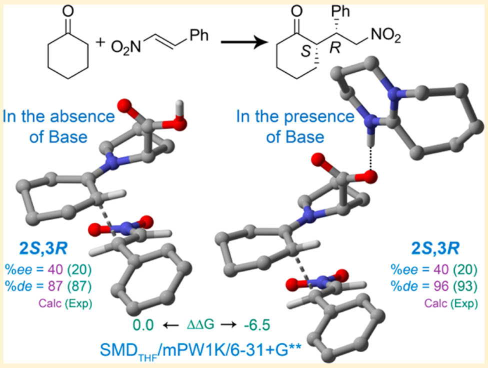

■ INTRODUCTION

The area of organocatalysis continues to witness consistent growth both in methodological developments as well as in its applications.[1] A plethora of organic reactions such as aldol, Michael, Mannich, *α*-amination, *α*-aminoxylation, and so on constitute the repertoire of organocatalytic protocols. While several catalysts emerged through these developmental strides spanning over a decade, proline and other pyrrolidines enjoy the highest level of acceptance.[2] The early impetus to proline catalysis offered by mechanistic insights obtained through computational studies is invaluable.[3] In particular, the transition-state (TS) models centered on enamine intermediates have been quite successful toward rationalizing the stereochemical outcome in proline-catalyzed reactions.[4] There have been interesting experimental studies aimed at establishing the identity of pivotal intermediates, such as enamine, iminium, and oxazolidinones in proline catalysis.[5] The presence of more readily detectable oxazolidinones has recently motivated alternative TS models invoking the *anti*-face approach of the incoming electrophile with respect to the carboxylic acid group.[6]

Recent studies from our laboratory demonstrated that the TS for the *syn*-face addition of enamine−carboxylic acid to the electrophile (also known as the Houk−List model) is the most preferred mode in aldol reactions,[7a] while *anti*-face addition involving the Seebach−Eschenmoser TS model yields enantioselectivities in accordance with the experimental observations for proline-catalyzed *α*-amination reaction under basic reaction conditions.[7b] However, similar studies comparing the suitability of these TS models in a Michael addition are not yet reported. The generally accepted TS model for proline-catalyzed Michael additions relies on hydrogen-bonding interactions between the carboxylic acid and the incoming electrophile.[8] For instance, under polar protic reaction conditions, such as in methanolic solvents, the transition-state model suitable for rationalizing the stereochemical outcome has been suggested to involve *syn*-face addition with two explicitly bound methanol molecules.[9] However, the validity of TSs involving *syn*-face approach of the electrophile under aprotic reaction conditions has not been examined. Similarly, under basic conditions where enamine carboxylate is more likely to be the key intermediate, instead of enaminecarboxylic acid, the validity of hydrogen-bonding TS model demands further scrutiny.

Herein we disclose some interestingly new insights on a proline-catalyzed Michael reaction between nitrostyrene and cyclohexanone, obtained through density functional theory computations using the mPW1K and B3LYP functionals in conjunction with the 6-31+G** basis set (Scheme 1). Solvent effects are included using the SMD_{THF}/mPW1K/6-31+G** level of theory. The discussions are presented on the basis of the Gibbs free energies obtained at the SMD_{THF}/mPW1K/6-31+G** level of theory, including thermal and entropic

Received: October 24, 2012
Published: November 27, 2012

dx.doi.org/10.1021/jo3023654 | *J. Org. Chem.* 2012, 77, 10516−10524

Scheme 1. Proline-Catalyzed Michael Reaction[6]

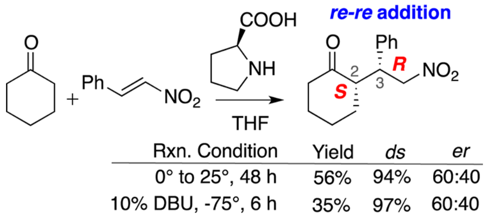

Rxn. Condition	Yield	*ds*	*er*
0° to 25°, 48 h	56%	94%	60:40
10% DBU, -75°, 6 h	35%	97%	60:40

corrections at 298 K for each stationary point in THF continuum. Emphasis has been placed on the ability of each TS model to reproduce the experimentally observed enantio- and diastereoselectivities of the title reaction.

■ COMPUTATIONAL METHODS

Geometries of all stationary points were optimized by using the Gaussian09 suite of quantum chemical programs.[10] The transition states (TS) and minima were first located at the mPW1K/6-31+G** and the B3LYP/6-31+G** levels of theory in the gas phase.[11] The effect of solvent was taken into account by optimization of all geometries at the SMD_{THF}/mPW1K/6-31+G** level of theory.[12] The lower energy TSs in different TS models were subjected to additional geometry optimizations at the SMD_{THF}/M06-2X/6-31+G** level of theory.[13] The B3LYP functional has been known to perform quite well for asymmetric organocatalyzed reactions, especially in proline-catalyzed reactions.[14] However, it has been questioned for its ability to account for weak van der Waals interactions (dispersion interaction).[15] We have used the mPW1K functional owing to its ability toward estimating the barrier heights as well as other kinetic parameters.[16] In addition, the M06-2X functional is employed for a set of crucial TSs in each model examined. The performance of the M06-2X functional has been assessed as being suitable for obtaining improved estimates on noncovalent interactions as well as for thermochemical and kinetic parameters.[17]

All of the stationary points were characterized by frequency calculations to confirm either as a minimum or a first-order saddle point (TS). The one and only one imaginary frequency of the TS was verified as corresponding to the desired reaction coordinate at each level of theory employed in this study. A representative set of TSs in each model was further verified by using the intrinsic reaction coordinate (IRC) calculation at $\text{SMD}_{\text{(THF)}}$/mPW1K/6-31+G** level of theory.[18] The IRC trajectories thus generated are provided in the Supporting Information (Figure S18). The energies employed for discussions in the text are the Gibbs free energies obtained at the $\text{SMD}_{\text{(THF)}}$/mPW1K/6-31+G** level of theory.[19] The Gibbs free energies ($\Delta G_{298\text{K}}$) were calculated by using the standard statistical mechanical treatment (within the rigid rotor and harmonic oscillator approximations) wherein the entropic and thermal corrections are included.

Topological analysis of the electron densities, within Bader's Atoms-in-Molecule (AIM) framework, was carried out by using AIM2000 software.[20] AIM analyses were performed on the geometries obtained at the SMD_{THF}/mPW1K/6-31+G** level of theory. The *activation strain analysis* was performed to calculate the extent of distortion in the TSs.[21] According to the activation strain model, the activation energy E_{act} is considered as consisting of two components, $E_{\text{strain/distortion}}$ (distortion (or strain) energy) and E_{int} (interaction).

$$E_{\text{act}} = E_{\text{int}} + E_{\text{strain}}$$

The $E_{\text{strain/distortion}}$ is the energy difference between the energy of the unstrained reactants, namely enamine and nitrostyrene, and their energy in the TS in the distorted form. The E_{strain} gives the measure of distortion in the substrate geometry in the TS. The energy of the distorted reactants in the TS was computed by evaluating single point energies of the distorted geometry of enamine and nitrostyrene fragments as noticed in the TS.

$$E_{\text{strain/distortion}} = (E_{\text{enamine(TS)}} + E_{\text{nitrostyrene(TS)}}) - (E_{\text{enamine}} + E_{\text{nitrostyrene}})$$

The interaction energy (E_{int}) is the binding interaction between the distorted reactants as noticed the TS geometry. The E_{int} was calculated as

$$E_{\text{int}} = E_{\text{(TS)}} - (E_{\text{enamine(TS)}} + E_{\text{nitrostyrene(TS)}})$$

■ RESULTS AND DISCUSSION

One of the key control elements invoked in the conventional TS model for the stereoselective C−C bond formation is the H-bonding stabilization of the developing negative charge on the electrophile by the proline −COOH group. For example, the stabilization offered by the −COOH group to a developing alkoxide in an aldol transition state as the C−C bond formation occurs is expected to be significant owing the lack of other delocalizations of the incipient charge on the oxygen atom. The efficiency of delocalization of the developing charges in the TS would naturally vary depending on the nature of the electrophile. Michael addition offers an interesting example for probing the significance of hydrogen bonding offered by the carboxylic acid due to the key differences with the other proline-catalyzed reactions as summarized herein. This is due to (a) the fluxionality of the pyrrolidine ring, (b) the presence of two additional atoms between the site of enamine attack and the oxygen atom of the $-NO_2$ group interacting with the −COOH, (c) the stabilization of the developing negative charge by the electron withdrawing $-NO_2$ group there by diminishing the need for H-bonding stabilization, and (d) the lack of transfer of proton to the electrophile in the C−C bond forming step. In 1,4-additions such as the Michael addition, nitrostyrene can therefore approach the enamine through the face *anti* to the −COOH and at the same time enjoy the aforementioned stabilizing H-bonding interaction. These features of the TS are in stark contrast with the other organocatalytic reactions such as aldol, α-amination, and α-aminoxylation, wherein approach of the electrophile from the face *anti* to −COOH is known to be much less favored.[22] The effect of these contributing factors in controlling the stereochemical course of asymmetric Michael addition (Scheme 2) is presented in the following sections.

In conformity with the widely accepted mechanism, a reactive nucleophilic enamine intermediate is considered to

Scheme 2. Stereocontrolling C−C Bond Formation between Nitrostyrene and (a) Enaminecarboxylic Acid (1) or (b) Enaminecarboxylate (3), Respectively, in the Absence and Presence of a Base

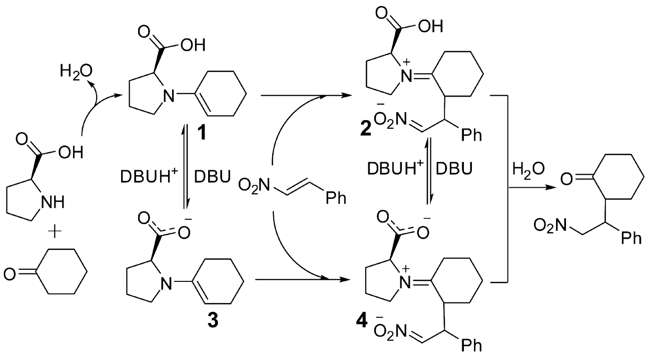

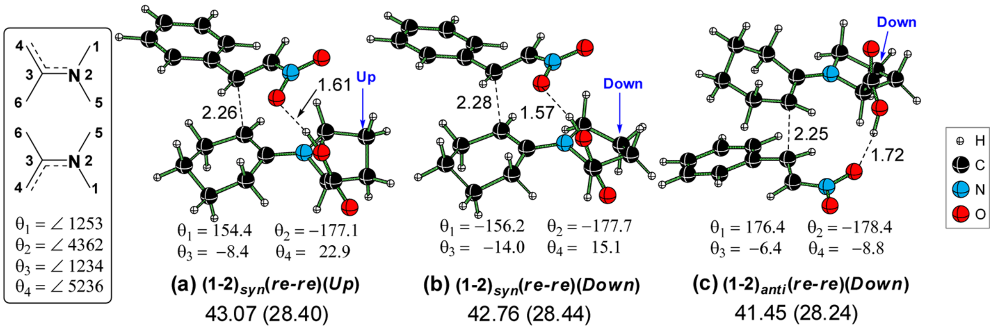

(a) $\mathbf{(1\text{-}2)}_{syn}$***(re-re)(Up)*** 43.07 (28.40)

(b) $\mathbf{(1\text{-}2)}_{syn}$***(re-re)(Down)*** 42.76 (28.44)

(c) $\mathbf{(1\text{-}2)}_{anti}$***(re-re)(Down)*** 41.45 (28.24)

Figure 1. Optimized geometry of the **TS(1−2)** for the *re-re* mode of addition for *up* and *down* pyrrolidine ring conformations in *syn*-face (**a**, **b**) and *anti*-face (**c**) additions. The relative Gibbs free energies (in kcal/mol) are with respect to the separated reactants at the SMD$_{\mathrm{THF}}$/mPW1K and SMD$_{\mathrm{THF}}$/M06-2X (in parentheses). Distances are in angstroms and angles in degrees.

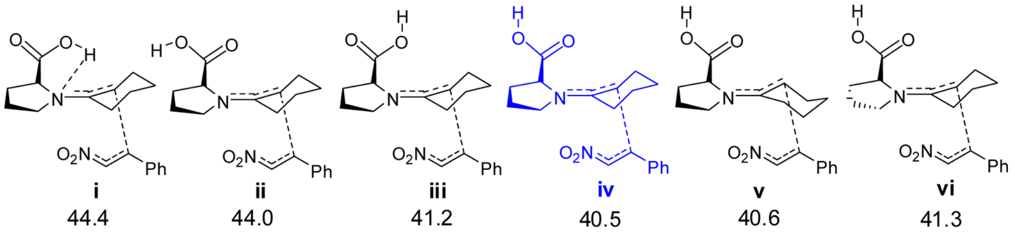

Figure 2. Various conformers of the C−C bond formation transition state **TS(1−2)′** in the *re-re* mode of approach between enamine and nitrostyrene. The relative Gibbs free energies (in kcal/mol) are with respect to the separated reactants at the SMD$_{\mathrm{THF}}$/mPW1K level of theory.

have generated between cyclohexanone and proline. The enamine thus formed can react with the electrophile in stereochemically different modes, depending on the prochiral faces. All prochiral approaches between the enamine and nitrostyrene such as *re-re*, *re-si*, *si-re*, and *si-si* are examined. The transition-state notations such as *re-re* imply the addition of the *re*-face of enamine on the *re*-face nitrostyrene. For transition states, devoid of any interaction between $-NO_2$ and −COOH, three dihedral angles (60°, 180°, and 300°) with respect to the enamine double bond are considered. Also two different conformations, each for pyrrolidine and cyclohexyl rings, are considered in the TS. In the TS involving H-bonding interaction, the interaction of −COOH with each O-atom of the NO_2-group of nitrostyrene is also examined.

First, *syn*-face addition of enamine **1**, denoted as $\mathbf{(1-2)}_{syn}$, is considered. In the *syn*-face addition, the approach of nitrostyrene is from the same face as that of the carboxylic acid group. Two key ring conformers, '*up*' and '*down*' that differ in terms of the relative positions of pyrrolidine C4 methylene group is examined (Figure 1). The comparison of energies between *re-re*, *re-si*, *si-re*, and *si-si* modes of addition indicates that the *re-re* addition in the case of *down* conformer is of the lowest relative Gibbs free energy. In this group of *syn*-face addition TSs, the *up* conformer is lower in energy for other stereochemical modes of approach between enamine and nitrostyrene. Also among the puckered cyclohexane ring conformers, the TS with the C4 methylene of cyclohexane toward the incoming electrophile is of lower in energy. If C_4 remains away from the incoming electrophile, the axial C−H of C3 methylene will point toward the incoming electrophile causing an increased steric interaction near the site of C−C bond formation. While the *re-re* stereochemical mode corresponds to the experimentally reported major diastereomer, the TS responsible for the enantiomeric product, namely *si-si* mode, is found to be 2.6 kcal/mol higher in energy. An energy difference of this order is at variance with the low enantiomeric ratio of 60:40 noted experimentally. The origin of the energy separation between these diastereomeric TSs is traced to the differences in the efficiency of hydrogen bonding as well as the distortion within each reacting partner accompanying the bond formation (*vide infra*). In the case of *down* conformer, improved H-bonding as well as reduced distortion is noticed in the *re-re* mode of addition (Figure 1(**b**)). The distortion in the TS for the *si-si* mode of addition is identified as higher than that in *re-re* rendering larger difference in their energies.

As discussed earlier, due to the fluxionality of the pyrrolidine ring and the fact that the site of enamine attack and the oxygen atom of the $-NO_2$ group are away by two atoms, the hydrogen bonding interaction between the $-NO_2$ the −COOH groups continues to remain feasible even in the *anti*-face addition. The geometry of the most preferred TS in this family is provided in Figure 1(c). It is noticed that the hydrogen bonding between the $-NO_2$ the −COOH groups does exist, though it is relatively weaker than that in the case of *syn*-face approach. Interestingly, the TS energy for the *re-re* addition is found to be lower than that in the corresponding *syn*-face addition, suggesting that this model can account for the formation of the major diastereomer.[23] However, the difference between the lowest energy TS and its diastereomeric partner (*si-si* mode) is 3.9 kcal/mol, which evidently results in an overestimation of the enantiomeric ratio.[24] In spite of weaker H-bonding in the *anti*-face addition TS, it is lower in energy than the *syn*-face addition due to reduced distortion in the enamine moiety, as evident from a relatively more planar enamine in $\mathbf{(1-2)}_{anti}$(*re-re*). In the case of *syn*-face addition, the pyrrolidine nitrogen becomes more pyramidal so as to create more room for enabling a favorable H-bonding (θ_1 in Figure 1).

Some of the very successful *α*-substituted secondary amine catalysts employed in asymmetric Michael reactions, such diphenylmethylsilylethers, do not contain effective hydrogen bonding groups as that in proline. The transition state models

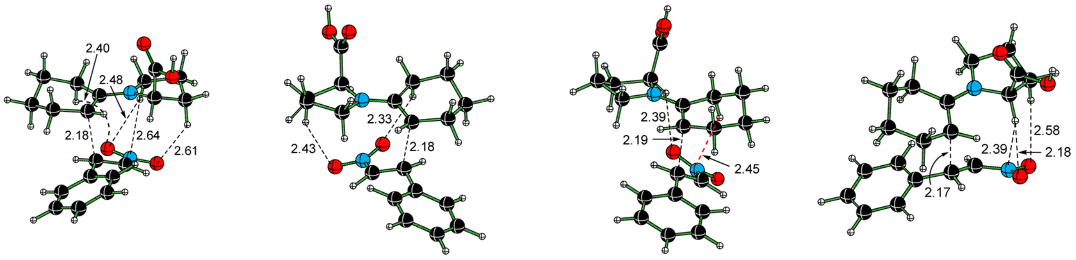

(1-2)′$_{anti}$ (*re-re*)$_{60}$ 40.47 (26.03) **(1-2)′**$_{anti}$ (*si-si*)$_{300}$ 40.99 (26.15) **(1-2)′**$_{anti}$ (*si-re*)$_{60}$ 42.07 (28.84) **(1-2)′**$_{anti}$ (*re-si*)$_{60}$ 42.73 (29.36)

Figure 3. Optimized geometry of four of the lower energy **TS(1−2)′** for the *anti*-face addition devoid of H-bonding with the carboxylic acid. The relative Gibbs free energies (in kcal/mol) are with respect to the separated reactants at the SMD_{THF}/mPW1K and SMD_{THF}/M06-2X (in parentheses). Distances are in angstroms.

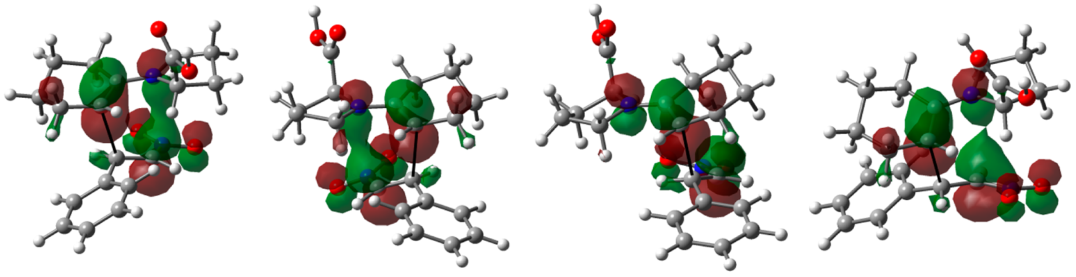

(1-2)′$_{anti}$ (*re-re*)$_{60}$ **(1-2)′**$_{anti}$ (*si-si*)$_{300}$ **(1-2)′**$_{anti}$ (*si-re*)$_{60}$ **(1-2)′**$_{anti}$ (*re-si*)$_{60}$

Figure 4. Secondary orbital interactions noticed in the HOMO of the TS for the C−C bond formation obtained at the $SMD_{(THF)}$/mPW1K/6-31+G** level of theory. The contours are generated with a uniform value of 0.04.

for pyrrolidines with large α-substituents invokes an *anti*-face addition wherein the electrophile approaches from the face opposite to that of the bulky group.[25] In this backdrop, the possible involvement of an *anti*-face approach (**(1−2)′**$_{anti}$) of nitrostyrene to the proline-cyclohexenyl enamine devoid of any interaction between −COOH and $-NO_2$ groups is examined.[26] Careful consideration of various conformational possibilities arising due to the rotation of −COOH, pyrrolidine, and cyclohexenyl ring puckering is done for the *re-re* mode of addition, as illustrated in Figure 2. Although for **TS(1−2)′** conformers **iv** and **v** are nearly degenerate, conformer **iv** is found to be slightly lower in energy for other stereochemical modes of approach such as *si-si*, *si-re*, *re-si*.[27] The most preferred conformer of **TS(1−2)′** is retained in other stereochemical modes of additions as well.[28]

The optimized geometries of stereocontrolling lower energy TSs are provided in Figure 3. While the orientation of the carboxylic acid is away from the developing charge on the nitro group to have offered hydrogen-bonding stabilization, other weak interactions between the nitro group and the methylene C−H moieties of pyrrolidine and cyclohexenyl rings can be noticed.

The most interesting aspect at this juncture is that the TSs such as **TS(1−2)′** involved in the *anti*-face addition, devoid of any H-bonding between −COOH and $-NO_2$, are lower in energy than the conventional H-bonding TS model **TS(1−2)**. **TS(1−2)′** is preferred by about 1 kcal/mol at the SMD_{THF}/mPW1K level of theory and 2.2 kcal/mol at the SMD_{THF}/M06-2X level of theory. In this TS model, the lowest energy **TS(1−2)′**(*re-re*)$_{60}$ corresponds to 2*S*,3*R* product configuration in concurrence with the experimentally observed major stereoisomer. Gratifyingly, the energy difference between TSs for the *re-re* and *si-si* additions in this model is as low as 0.5 kcal/mol, which in turn, is consistent with the low observed enantiomeric ratio. In general, the *anti*-face TS model devoid of H-bonding offers % ee and % de quite close to that of the experimental observations (vide infra). This prediction is highly suggestive of a non-hydrogen bonding TS as holding the key to stereoselectivity under aprotic reaction conditions.

In an effort to rationalize the predicted trends, the stereoelectronic features of the TSs are carefully analyzed. A number of differential stabilizing interactions are identified in these TSs as compared to the earlier TS-models involving H-bonding between −COOH and $-NO_2$ (Figure 3). The TS exhibiting shorter contact between the nitrogen atoms of pyrrolidine and nitrostyrene (such as that in *re-re* and *si-si* modes) are found to be of lower energy. Apart from the primary orbital interaction, leading to the new C−C bond between the enamine and nitrostyrene moieties, these TSs are also identified to enjoy a secondary orbital interaction between the depleting nitrogen lone pair of the enamine moiety and π^* of the developing C=N bond of the nitrostyrene as shown in Figure 4.[29] In the case of TSs involving *re-si* and *si-re* modes of addition, the NO_2 group is positioned in a less favorable position for secondary orbital interaction. These latter modes are of higher energy as compared to *re-re* and *si-si* modes. A stabilizing interaction of $-NO_2$ group with the α-CH of pyrrolidine and cyclohexane rings are also identified. The nature of these weak interactions is further characterized by using Atoms-in-Molecule (AIM) analysis.[30] In *si-re* and *re-si* TSs, a relatively weaker interaction between $-NO_2$ and pyrrolidine ring is noticed. The cumulative effect of all these differential interactions contributes to the high diastereoselectivity.

The quantification of distortion in and interaction between the reacting partners using the *activation strain* analysis on the above-mentioned TS models helped us gain additional insights. The conventional H-bonding TS model, **TS(1−2)**, is identified to encounter enhanced distortion/strain (>2 kcal/mol) while attempting to maintain H-bonding interaction between the $-NO_2$ and $-COOH$ groups. For instance, the activation strain energy ($E^{\ddagger}_{\text{strain}}$) for the *re-re* mode of addition in **TS(1−2)**$_{anti}$(*down*) is higher by 2.2 kcal/mol than that in **TS(1−2)′**$_{anti}$(*up*). A closer look at the data provided in Table 1 reveals that higher degree of distortion in **TS(1−2)** originates from the enhanced distortion in the enamine moiety. The distortion energy of enamine in **TS(1−2)′** falls in the range of 10 to 12 kcal/mol whereas it is more than 13 kcal/mol in the case of **TS(1−2)**. This implies that the advantage of the additional stabilization offered by the H-bonding interaction is nearly counter-balanced by higher geometric strain in the TS. This analysis further helps identify that in **TS(1−2)**, the *si-si* mode has higher distortion than in the *re-re* mode, causing larger energy separation between the stereocontrolling TSs. For example, $\Delta E^{\ddagger}_{\text{strain}}$ in **TS(1−2)**$_{syn}$(*si-si*)(*up*) is higher by 4 kcal/mol as compared to that in **TS(1−2)**$_{anti}$(*re-re*)(*down*). This could be regarded as the origin of overestimation in the computed enantioselectivity, when conventional H-bonding TS model is employed. The activation strain analysis further confirms that in **TS(1−2)** *anti*-face addition for the *re-re* mode is more preferred over the corresponding *syn*-face addition due to higher distortion (∼2 kcal/mol) in the latter case. For **TS(1−2)′**$_{anti}$, the *si-si* mode is of higher energy than the *re-re* mode due to slightly higher strain in nitrostyrene (0.7 kcal/mol), as the pyrrolidine ring in the *si-si* mode is not in a preferred conformation to interact with the $-NO_2$ group (Table 1). In the TS(**1−2**)′$_{anti}$ for *re-si* and *si-re* modes of addition the larger distrotion and reduced interaction between the reacting partners is identified as the reason for their higher energy.

Table 1. Summary[a] of Activation-Strain Analysis for the Lowest Energy TS from Different TS Models Obtained at the SMD_{THF}/mPW1K/6-31+G Level of Theory**

mode of addition	$\Delta E^{\ddagger}_{\text{strain-enamine}}$	$\Delta E^{\ddagger}_{\text{strain-nitrostyrene}}$	$\Delta E^{\ddagger}_{\text{strain}}$	$\Delta E^{\ddagger}_{\text{int}}$	$\Delta E^{\ddagger}$
TS(1−2)$_{syn}$ (*up*)					
re-re	14.4	12.1	26.5	−10.6	15.9
si-si	16.9	11.7	28.6	−11.9	16.7
si-re	13.4	13.1	26.5	−11.3	15.2
re-si	14.6	12.4	27.0	−10.5	16.5
TS(1−2)$_{syn}$ (*down*)					
re-re	15.6	11.2	26.7	−11.2	15.5
si-si	18.0	12.3	30.3	−12.5	17.8
si-re	16.0	13.6	29.6	−11.8	17.7
re-si	17.2	14.0	31.2	−15.4	15.7
TS(1−2)$_{anti}$ (*down*)					
re-re	13.6	11.0	24.6	−11.0	13.6
si-si	22.2	10.4	32.6	−14.9	17.7
si-re	21.3	12.9	34.1	−13.0	21.1
re-si	15.2	11.6	26.8	−11.1	15.7
TS(1−2)′$_{anti}$ (*up*)					
re-re	9.8	12.6	22.4	−9.1	13.3
si-si	9.4	13.3	22.7	−8.9	13.8
si-re	10.0	13.1	23.1	−7.3	15.8
re-si	11.8	13.8	25.6	−9.4	16.2

[a] The energies are calculated with respect to the separated lowest energy enamine+nitrostyrene. The energies are in kcal/mol.

One more vital aspect pertaining to the TS models employed in proline-catalyzed Michael additions can be noted as follows. In general, the stereocontrolling TSs are assumed to be the same for both basic and base-free reaction conditions. Particularly significant are the potential changes in the mechanistic features when the nature of the active nucleophile is changed. It is therefore of importance to examine whether (a) the active catalytic species is an enamine carboxylic acid or a deprotonated enamine carboxylate, (b) explicit inclusion of base in the TS model is desirable or not, (c) *syn*- or *anti*-face addition is more favored. Each of these factors can have a direct impact on the stereochemical outcome of the reaction. In the following section, we attempt to answer these questions on the basis of the computed relative energies of the TSs.

Under basic reaction conditions, enamine carboxylic acid could remain as enamine carboxylate. In view of such possibilities, we have evaluated the energetics for the addition of enamine carboxylate (**3**) to nitrostyrene (Figure 5). The *anti*-face addition is predicted to be more preferred in this case.[31] The diastereo- and enantioselectivities could be effectively rationalized by using such *anti*-face addition TS models. However, these TSs are higher in energy than that involving the corresponding enamine carboxylic acid (**1**). For instance, the Gibbs free energy of the lowest energy TS in this group **TS(3−4)**$_{anti}$(*re-re*)$_{60}$ is 1.7 kcal/mol higher than the enamine carboxylic acid pathway via **TS(1−2)′**$_{anti}$(*re-re*)$_{60}$, implying that this pathway is less likely be responsible for the stereochemical outcome of the reaction.

Another TS model with an explicitly bound DBU-H^+, as shown in Figure 6, is also considered. In a very recent report, Gschwind and co-workers have employed in situ NMR techniques to establish the presence of prolinate-DBU-H^+ ion

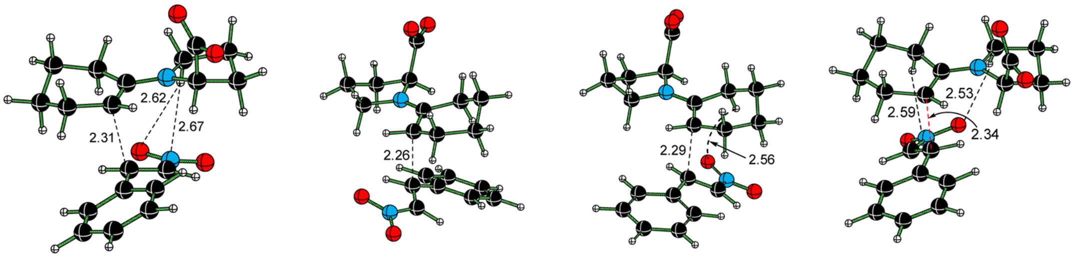

(3-4)$_{anti}$ (*re-re*)$_{60}$
42.16 (29.93)

(3-4)$_{anti}$ (*si-si*)$_{180}$
42.35 (30.42)

(3-4)$_{anti}$ (*si-re*)$_{60}$
44.11 (31.76)

(3-4)$_{anti}$ (*re-si*)$_{300}$
44.23 (34.17)

Figure 5. Optimized geometry of **TS(3−4)** for the C−C bond formation. The relative Gibbs free energies are with respect to the separated reactants at SMD_{THF}/mPW1K and SMD_{THF}/M06-2X (in parentheses). Distances are in angstroms.

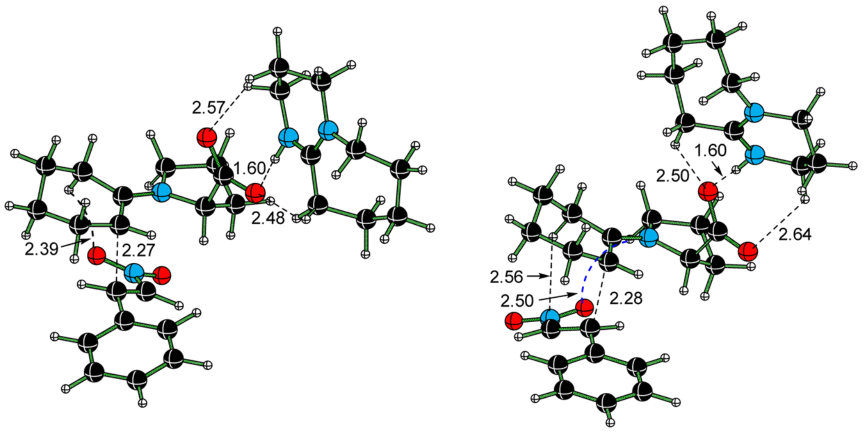

(3-4)$_{\mathbf{DBU}\text{-}\mathbf{\mathit{anti}}}$ (*re-re*)$_{60}$
33.98 (19.09)

(3-4)$_{\mathbf{DBU6}\text{-}\mathbf{\mathit{anti}}}$ (*re-si*)$_{300}$
36.49 (22.79)

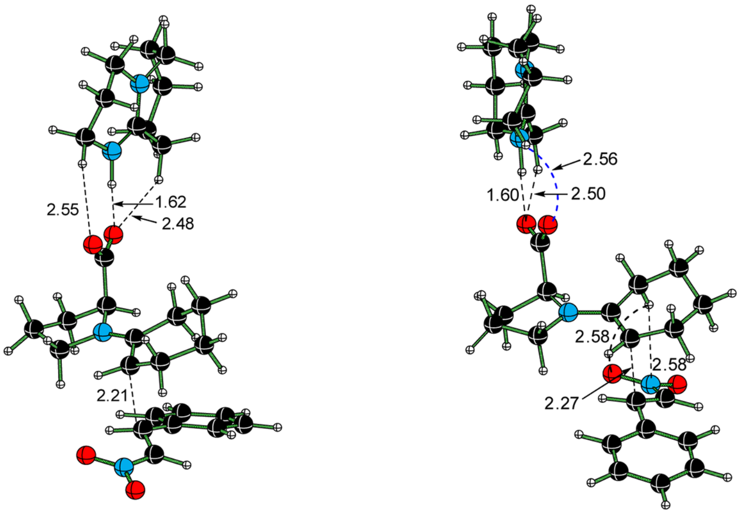

(3-4)$_{\mathbf{DBU}\text{-}\mathbf{\mathit{anti}}}$ (*si-si*)$_{180}$
34.51 (20.06)

(3-4)$_{\mathbf{DBU}\text{-}\mathbf{\mathit{anti}}}$ (*si-re*)$_{60}$
36.32 (22.78)

Figure 6. Optimized geometry of **TS(3−4)**$_{\mathbf{DBU}}$ for the C−C bond formation for different modes of addition. The relative Gibbs free energies (in kcal/mol) are with respect to the separated reactants at the SMD$_{\mathrm{THF}}$/mPW1K and SMD$_{\mathrm{THF}}$/M06-2X (in parentheses). Distances are in angstroms.

pair.[32] In the present study, first, different sites of interaction of protonated DBU with the substrate are examined. Subsequently, all the key conformers of **3-DBU**-H$^+$ adduct (**3**$_{\mathbf{DBU\text{-}H+}}$) and corresponding TS for the (*re-re*)$_{60}$ mode is probed.[33] The **3**$_{\mathbf{DBU}}$ adduct is lower in energy than separated **1** and **DBU** (ΔG = −1.9, ΔH = −11.2 kcal/mol). The lowest energy TS in this model **TS(3−4)**$_{\mathbf{DBU}\text{-}\mathbf{\mathit{anti}}}$(*re-re*)$_{60}$ is 6.5 kcal/mol lower than **TS(1−2)**$'_{\mathit{anti}}$(*re-re*)$_{60}$. The H-DBU$^+$-bound TSs enjoy additional stabilization, particularly due to the specific interaction between the carboxylate group and DBU-H$^+$. The optimized geometries of important stereochemical modes of addition are shown in Figure 6. Any such specific interaction, either with solvent molecules or with an additive such as DBU, as in the present situation, is inadequately represented in a continuum solvation treatment.[34] In addition to the stabilization offered by the H-bonding between **3** and DBU-H$^+$, the **TS(3−4)**$_{\mathbf{DBU}\text{-}\mathbf{\mathit{anti}}}$ is also identified to exhibit relatively reduced strain in the enamine-DBU adduct as compared to that of enamine in **TS(1−2)**$'$, which renders improved stability to **TS(3−4)**$_{\mathbf{DBU}\text{-}\mathbf{\mathit{anti}}}$. Such additional stabilization of the TS as noted herein can result in faster reaction rate in the presence of a base such as DBU. In fact, at lower temperatures, the reaction is known to proceed faster in the presence of DBU (see Scheme 1).[35]

The computed relative energies of different transition states in the **TS(3−4)**$_{\mathbf{DBU}}$ family with respect to the lowest energy *re-re* mode of addition are summarized in Table 2. It can be readily noticed that the difference between the *re-re* and *si-si* modes of additions at the SMD$_{\mathrm{THF}}$/mPW1K level of theory are less than half a kcal/mol, which corresponds to a very low enantiomeric excess. This prediction is in good accordance with the experimental %ee of 20. However, the SMD$_{\mathrm{THF}}$/M06-2X energetics results in overestimation of the enantiomeric excess. Similarly, the predicted diastereomeric excess using the M06-2X energies is also found to be higher as compared to the experimental values. The SMD$_{\mathrm{THF}}$/mPW1K method provides improved estimates of stereoselectivity than that obtained using the SMD$_{\mathrm{THF}}$/M06-2X method.

The stereoselectivity can be rationalized using similar factors as described earlier in the case of **TS(1−2)**$'$. The higher energy TSs involving *si-re* and *re-si* modes lack interaction between the $-NO_2$ group of nitrostyrene and the pyrrolidine ring of

Table 2. Relative Energies[a] (in kcal/mol) of the Lowest Energy Transition States in Each Stereochemical Mode of Approach between Enamine and Nitrostyrene for TS(3−4)$_{DBU}$ and the Corresponding Stereoselectivity

	SMD$_{THF}$/mPW1K		SMD$_{THF}$/M06-2X	
TS(3−4)$_{DBU}$	$\Delta\Delta G$	$\Delta\Delta H$	$\Delta\Delta G$	$\Delta\Delta H$
re-re	0.0	0.0	0.0	0.0
si-si	0.5	0.4	1.0	1.2
si-re	2.3	2.3	3.7	4.5
re-si	2.5	3.0	3.7	4.5
%de (*S*,*R*)	96	96	>99	>99
%ee (*S*,*R*)	40	33	69	77

[a] Additional data is provided in Tables S9−S12 in the Supporting Information.

proline−enamine, besides positioning of the $-CH_2NO_2$ group of nitrostyrene below the cyclohexane ring causing higher steric interaction. The low interaction energy between the reactants in these TSs (*si-re* and *re-si* modes) is confirmed by the activation strain analysis (Table 3). Among the lower energy *re-re* and *si-si* modes of addition, reduced interaction between enamine and nitrostyrene in the TS as well as higher strain in the nitrostyrene fragment for the *si-si* mode of addition is noticed.

Table 3. Summary[a] of Activation-Strain Analysis for the Lowest Energy TS(3-4)$_{DBU\text{-}anti}$(*up*) Obtained at the SMD$_{THF}$/mPW1K/6-31+G Level of Theory**

mode of addition	$\Delta E^{\ddagger}_{\text{strain-enamine}}$	$\Delta E^{\ddagger}_{\text{strain-nitrostyrene}}$	$\Delta E^{\ddagger}_{\text{strain}}$	$\Delta E^{\ddagger}_{\text{int}}$	$\Delta E^{\ddagger}$
re-re$_{60}$	6.3	10.1	16.4	−8.6	7.7
si-si$_{180}$	5.8	11.2	17.0	−8.1	8.9
si-si$_{300}$	5.1	10.9	15.9	−8.1	7.8
si-re$_{60}$	5.2	10.3	15.5	−5.4	10.1
re-si$_{300}$	6.8	10.4	17.2	−6.4	10.8

[a] The energies calculated with respect to the separated reactants such as the lowest energy enamine−DBU adduct and nitrostyrene. The energies are in kcal/mol.

Now, a comparison between the efficiency of different TS models, thus far examined in this study, is presented. Two points are particularly noteworthy. The first one relates to the energetics of the C−C bond formation in different TS models and the other pertains to how successful a given model is toward arriving at the correct stereochemical outcome of the reaction. The computed relative energies, by taking the most preferred *re-re* mode of addition as a uniform reference, is provided in Table 4. It is readily evident that the **TS(3−4)$_{DBU\text{-}anti}$** consisting of a bound DBU-H$^+$ is energetically the most preferred model than other models such as the enamine carboxylic acid model (with no H-bonding) **TS(1−2)′$_{anti}$**. The TSs for *anti*-face addition, such as **TS(1−2)$_{anti}$**, exhibiting hydrogen bonding between the $-NO_2$ and −COOH groups, is much higher in energy.

The computed stereoselectivities both at the SMD$_{THF}$/mPW1K and SMD$_{THF}$/M06-2X levels of theory, together with the experimental values are compiled in Table 5. The TS models can be classified into two major groups. While **TS(1−2)** and **TS(1−2)′** are for base-free reaction conditions, the other set **TS(3−4)** and **TS(3−4)$_{DBU}$** involving deprotonated enamine carboxylic acid, are the models in the presence of DBU. It is conspicuous from the experimental observation that the inclusion of DBU brings hardly any change in the stereoselectivities, except for faster reaction rate. The predicted diastereoselectivities at the mPW1K level of theory are in good accord with the experimental observation. However, the low enantioselectivity can be rationalized only by invoking an *anti*-face addition, without the hydrogen bonding between the COOH and $-NO_2$ groups, such as in **TS(1−2)′**. Similarly, in the presence of DBU, the best estimates of enantioselectivity can be obtained through **TS(3−4)**. Since the H-DBU$^+$-bound TSs are energetically more preferred, it is highly likely that **TS(3−4)$_{DBU}$** holds the key to the stereochemical outcome of the title reaction.

Table 4. Relative Energies (in kcal/mol) of the Lowest Energy TS[a] in the *re-re* Mode of Addition for Different TS Models

	SMD$_{THF}$/mPW1K		SMD$_{THF}$/M06-2X	
TS	ΔG	ΔH	ΔG	ΔH
(1−2)$_{anti}$	41.45	24.10	28.24	10.67
(1−2)′$_{anti}$	40.47	23.98	26.03	8.71
(3−4)$_{anti}$	42.16	25.78	29.93	12.12
(3−4)$_{DBU\text{-}anti}$	33.98	7.13	19.09	−8.98

[a] Computed with respect to the ground-state reactants such as proline, cyclohexanone, and nitrostyrene as the common reference point. The lowest energy TS in each family (row) is chosen on the basis of the Gibbs free energies.

Table 5. Calculated % ee and % de Using the Gibbs Free Energies of Transition States from Various TS Models at Different Levels of Theory[a]

	% de		% ee	
TS model	L1	L2	L1	L2
base-free conditions				
(1−2)	85	47	>99	53
(1−2)′	87	98	40	8
in the presence of DBU				
(3−4)	93	91	17	40
(3−4)$_{DBU}$	96	>99	40	69
expt (no base)[b]	88		20	
expt (base)[b]	93		20	

[a] L1 = SMD$_{THF}$/mPW1K/6-31+G**; L2 = SMD$_{THF}$/M06-2X/6-31+G**. [b] The reaction time under base-free conditions is about 48 h while that with base is 6 h (ref 6).

■ CONCLUSION

The enantio- and diastereoselectivity issues in proline-catalyzed Michael reaction between cyclohexanone and nitrostyrene have been examined using various transition-state models for the stereocontrolling C−C bond formation step. The transition-state models, which differ in terms of the geometry of approach as well in the presence and absence of hydrogen-bonding interactions between the COOH group of proline and the $-NO_2$ group of nitrostyrene, have been examined. The predicted stereoselectivities using (a) *syn*- and *anti*-face approaches of nitrostyrene to enaminecarboxylic acid and (b) *anti*-face approach to enamine carboxylate are compared with the experimentally observed product distribution of the stereoisomers. In the closely related reactions such as in proline-catalyzed aldol, Mannich, α-aminoxylation, or α-aminations, it has been well-established that the preferred mode of approach of the electrophile is from the same face as that of the carboxylic acid owing to the vital hydrogen-bonding stabilization to the developing charges in the transition state offered by the proline carboxylic acid. However, the presence of an electron-withdrawing group in Michael acceptors, such as that in nitrostyrene, renders additional stabilization to the incipient charges accompanying the C−C bond formation in the transition state. The non-hydrogen bonding TS models involving the *anti*-face addition of enamine carboxylic acid or enamine carboxylate, respectively, under base-free and basic aprotic reaction conditions (with and without a bound DBU), have been found to be effective in rationalizing the enantio- and diastereo-selectivities. The TS models relying on the H-bonding stabilization between −COOH and $-NO_2$ groups respectively of proline-enamine and nitrostyrene in the stereocontrolling C−C bond formation are inadequate toward arriving at good estimates on the stereoselectivity for the title reaction. Furthermore, these TSs are of higher energy due to the increased strain/distortion of the enamine and nitrostyrene fragments in the TS. A H-DBU$^+$-bound transition state model involving *anti*-face approach of nitrostyrene to enamine carboxylate devoid of hydrogen bonding between −COOH and $-NO_2$ groups has been identified as energetically more favored over that without H-DBU$^+$. The ion-pair TS model has been identified as capable of rationalizing the stereochemical outcome as well as the rate-enhancements in the presence of DBU in proline-catalyzed Michael reactions.

■ ASSOCIATED CONTENT

Ⓢ Supporting Information

Optimized geometries, additional schemes, figures, and tables. This material is available free of charge via the Internet at http://pubs.acs.org.

■ AUTHOR INFORMATION

Corresponding Author

*E-mail: sunoj@chem.iitb.ac.in.

Notes

The authors declare no competing financial interest.

■ ACKNOWLEDGMENTS

Generous computing time from the IIT Bombay computer center is acknowledged. R.B.S. and A.K.S. are grateful to CSIR-New Delhi for funding (02(0052)/12/EMR-II) and a Senior Research Fellowship, respectively.

■ REFERENCES

(1) (a) Nielsen, M.; Worgull, D.; Zweifel, T.; Gschwend, B.; Bertelsen, S.; Jørgensen, K. A. *Chem. Commun.* **2011**, *47*, 632. (b) Bertelsen, S.; Jørgensen, K. A. *Chem. Soc. Rev.* **2009**, *38*, 2178;(c) *Chem. Rev.* **2007**, *107*, 12 special issue on organocatalysis. (d) Jacobsen, E. N.; MacMillan, D. W. C. *Proc. Natl. Acad. Sci. U.S.A.* **2010**, *107*, 20618.

(2) Mukherjee, S.; Yang, J. W.; Hoffmann, S.; List, B. *Chem. Rev.* **2007**, *107*, 5471.

(3) (a) Clemente, F. R.; Houk, K. N. *Angew. Chem., Int. Ed.* **2004**, *43*, 5766. (b) Hoang, L.; Bahmanyar, S.; Houk, K. N.; List, B. *J. Am. Chem. Soc.* **2003**, *125*, 16.

(4) (a) Cheong, P. H.-Y.; Legault, C. Y.; Um, J. M.; Çelebi-Ölçüm, N.; Houk, K. N. *Chem. Rev.* **2011**, *111*, 5042. (b) Sunoj, R. B. *WIREs Comput. Mol. Sci.* **2011**, *1*, 920.

(5) (a) Schmid, M. B.; Zeitler, K.; Gschwind, R. M. *Angew. Chem., Int. Ed.* **2010**, *49*, 4997. (b) Bock, D. A.; Lehmann, C. W.; List, B. *Proc. Natl. Acad. Sci. U.S.A.* **2010**, *107*, 20636. (c) Marquez, C.; Metzger, J. O. *Chem. Commun.* **2006**, 1539. (d) List, B.; Hoang, L.; Martin, H. J. *Proc. Natl. Acad. Sci. U.S.A.* **2004**, *101*, 5839.

(6) Seebach, D.; Beck, A. K.; Badine, D. M.; Limbach, M.; Eschenmoser, A.; Treasurywala, A. M.; Hobi, R.; Prikoszovich, W.; Linder, B. *Helv. Chim. Acta* **2007**, *90*, 425.

(7) (a) Sharma, A. K.; Sunoj, R. B. *Angew. Chem., Int. Ed.* **2010**, *49*, 6373. (b) Sharma, A. K.; Sunoj, R. B. *Chem. Commun.* **2011**, *47*, 5759.

(8) (a) Enders, D.; Seki, A. *Synlett* **2001**, 26. (b) Shinisha, C. B.; Sunoj, R. B. *Org. Biomol. Chem.* **2008**, *6*, 3921. (c) A suggestion on non-hydrogen-bonding models has also been made recently. See: Yang, H.; Wong, M. W. *Org. Biomol. Chem.* **2012**, *10*, 3229.

(9) Patil, M. P.; Sunoj, R. B. *Chem.—Eur. J.* **2008**, *14*, 10472.

(10) Gaussian 09, Revision A.02: Frisch, M. J.; Trucks, G. W.; Schlegel, H. B.; Scuseria, G. E.; Robb, M. A.;Cheeseman, J. R.; Scalmani, G.; Barone, V.; Mennucci, B.; Petersson, G. A.; Nakatsuji, H.; Caricato, M.; Li, X.; Hratchian, H. P.; Izmaylov, A. F.; Bloino, J.; Zheng, G.; Sonnenberg, J. L.; Hada, M.; Ehara, M.; Toyota, K.; Fukuda, R.; Hasegawa, J.; Ishida, M.; Nakajima, T.; Honda, Y.; Kitao, O.; Nakai, H.; Vreven, T.; Montgomery, J. A., Jr.; Peralta, J. E.; Ogliaro, F.; Bearpark, M.; Heyd, J. J.; Brothers, E.; Kudin, K. N.; Staroverov, V. N.; Kobayashi, R.; Normand, J.; Raghavachari, K.; Rendell, A.; Burant, J. C.; Iyengar, S. S.; Tomasi, J.; Cossi, M.; Rega, N.; Millam, N. J.; Klene, M.; Knox, J. E.; Cross, J. B.; Bakken, V.; Adamo, C.; Jaramillo, J.; Gomperts, R.; Stratmann, R. E.; Yazyev, O.; Austin, A. J.; Cammi, R.; Pomelli, C.; Ochterski, J. W.; Martin, R. L.; Morokuma, K.; Zakrzewski, V. G.; Voth, G. A.; Salvador, P.; Dannenberg, J. J.; Dapprich, S.; Daniels, A. D.; Farkas, Ö.; Foresman, J. B.; Ortiz, J. V.; Cioslowski, J.; Fox, D. J. Gaussian, Inc., Wallingford, CT, 2009.

(11) For the basis set, see: (a) Hehre, W. J.; Ditchfield, R.; Pople, J. A. *J. Chem. Phys.* **1972**, *56*, 2257. (b) Hariharan, P. C.; Pople, J. A. *Theor. Chim. Acta* **1973**, *28*, 213. For B3LYP, see: (c) Lee, C.; Yang, W.; Parr, R. G. *Phys. Rev. B* **1988**, *37*, 785. (d) Becke, A. D. *J. Chem. Phys.* **1993**, *98*, 5648. For mPW1K, see: (e) Lynch, B. J.; Fast, P. L.; Harris, M.; Truhlar, D. G. *J. Phys. Chem. A* **2000**, *104*, 4811. (f) Lynch, B. J.; Zhao, Y.; Truhlar, D. G. *J. Phys. Chem. A* **2003**, *107*, 1384.

(12) Marenich, A. V.; Cramer, C. J.; Truhlar, D. G. *J. Phys. Chem. B* **2009**, *113*, 6378.

(13) Zhao, Y.; Truhlar, D. G. *Theor. Chem. Acc.* **2008**, *120*, 215.

(14) (a) Bahmanyar, S.; Houk, K. N. *J. Am. Chem. Soc.* **2001**, *123*, 12911. (b) Bahmanyar, S.; Houk, K. N.; Martin, H. J.; List, B. *J. Am. Chem. Soc.* **2003**, *125*, 2475. (c) Bahmanyar, S.; Houk, K. N. *Org. Lett.* **2003**, *5*, 1249. (d) Cheong, P. H.-Y.; Houk, K. N. *J. Am. Chem. Soc.* **2004**, *126*, 13912. (e) References 7 and 8b.

(15) (a) Woodcock., H. L.; Schaefer, H. F., III; Schreiner, P. R. *J. Phys. Chem. A* **2002**, *106*, 11923. (b) Schreiner, P. R.; Fokin, A. A.; Pascal, R. A., Jr.; de Meijere, A. *Org. Lett.* **2006**, *8*, 3635. (c) Zhao, J.; Truhler, D. G. *J. Chem. Theory Comput.* **2007**, *3*, 289. (d) Wodrich, M. D.; Corminboeuf, C.; Schreiner, P. R.; Fokin, A. A.; Schleyer, P. v. R. *Org. Lett.* **2007**, *9*, 1851. (e) Grimme, S.; Steinmetz, M.; Korth, M. *J. Chem. Theory Comput.* **2007**, *3*, 42.

(16) (a) Lingwood, M.; Hammond, J. R.; Hrovat, D. A.; Mayer, J. M.; Borden, W. T. *J. Chem. Theory Comput.* **2006**, *2*, 740. (b) Canepa, C. *J. Phys. Chem. B* **2003**, *07*, 4437. (c) Gilbert, T. M.; Bachrach, S. M. *Organometallics* **2007**, *26*, 2672. (d) Jones, G. O.; Guner, V. A.; Houk, K. N. *J. Phys. Chem. A* **2006**, *110*, 1216. (e) Roy, D.; Sunoj, R. B. *Org. Lett.* **2007**, *9*, 4873.

(17) (a) Zhao, Y.; Truhlar, D. G. *J. Chem. Phys.* **2006**, *125*, 194101. (b) Zhao, Y. *J. Chem. Theory Comput.* **2011**, *7*, 669.

(18) (a) Gonzalez, C.; Schlegel, H. B. *J. Chem. Phys.* **1989**, *90*, 2154. (b) Gonzalez, C.; Schlegel, H. B. *J. Phys. Chem.* **1990**, *94*, 5523.

(19) Marenich, A. V.; Cramer, C. J.; Truhlar, D. G. *J. Phys. Chem. B* **2009**, *113*, 6378.

(20) (a) Bader, R. F. W. *Atoms in Molecules: A Quantum Theory*; Clarendon Press: Oxford, 1990. (b) AIM2000 Version 2.0; Buro fur Innovative Software, SBKSoftware: Bielefeld, Germany, 2002. (c) Biegler-Konig, F.; Schonbohm, J.; Bayles, D. *J. Comput. Chem.* **2001**, *22*, 545. (d) Biegler-Konig, F.; Schonbohm, J. *J. Comput. Chem.* **2002**, *23*, 1489.

(21) (a) van Zeist, W. J.; Bickelhaupt, F. M. *Org. Biomol. Chem.* **2010**, *8*, 3118. (b) Legault, C. Y.; Garcia, Y.; Merlic, C. A.; Houk, K. N. *J. Am. Chem. Soc.* **2007**, *129*, 12664.

(22) The *anti*-addition to *syn*-enamine in the case of aldol and α-amination was found to be higher in energy (see ref 7). The addition of *anti*-enamine will be more unfavorable due to increased strain/distortion.

(23) A complete set of relative energies of **TS(1−2)** is provided in Table S1 in the Supporting Information. See Figures S3−S7 (Supporting Information) for optimized TS geometries.

(24) Under polar protic media such as in methanol, inclusion of explicit solvent molecules in the transition-state model was reported as being fruitful in arriving at the correct stereochemcial outcome for Michael addition reactions. See ref 9.

(25) Patil, M. P.; Sharma, A. K.; Sunoj, R. B. *J. Org. Chem.* **2010**, *75*, 7310 and ref 8b.

(26) (a) The *syn*-face approach of nitrostyrene $\mathbf{TS(1{-}2)'}_{syn}$ is found to be of higher energy than the *anti*-face approach. (b) The energies of different modes of addition for *anti*- and *syn*-face additions of nitrostyrene to enamine in **TS(1−2)′** are provided in Table S5 (Supporting Information). See Figures S9 and S10 (Supporting Information) for optimized TS geometries.

(27) For energies of two different TSs in **TS(1−2)′** family arising due to the cyclohexyl ring puckering in different modes of addition, see Table S4 (Supporting Information).

(28) Additional details on conformers are provided in Figures S8 and Tables S3-S4 in the Supporting Information.

(29) The role of secondary orbital interaction in organocatalytic Michael reactions has earlier been demonstrated as an important contributing factor in bringing about the vital energy separation desirable for stereoinduction. See ref 25.

(30) See Figures S19−S22 (Supporting Information) for additional details of bond paths between the interacting atoms and the corresponding electron densities at the bond critical points.

(31) See Table S7 and Figures S11 and S12 (Supporting Information) for further details.

(32) (a) Schmid, M. B.; Zeitler, K.; Gschwind, R. M. *Chem.—Eur. J.* **2012**, *18*, 3362. (b) Mayr and co-workers have also suggsted the participation of prolinate-DBU-H^+ ion pair in THF. See: Kanzian, T.; Lakhdar, S.; Mayr, H. *Angew. Chem., Int. Ed.* **2010**, *49*, 9526.

(33) (a) As many as eight different $\mathbf{3}_{\mathrm{DBU\text{-}H+}}$ adducts are considered for the (*re-re*)$_{60}$ mode of addition. See Figure S15 and Table S8 (Supporting Information). (b) The $\mathbf{3}_{\mathrm{DBU\text{-}H+}}$ involved in the lowest energy TS is considered further for all modes of addition. For the lowest energy TSs, see Figure S16 and Table S9 (Supporting Information) and for other related TSs, see Tables S10−S14 (Supporting Information).

(34) Sunoj, R. B.; Anand, M. *Phys. Chem. Chem. Phys.* **2012**, *14*, 12715.

(35) (a) Reference 6. (b) A TS wherein DBU-H^+ is bound to the NO_2 group has also been examined. However, such a TS is found to be higher in energy by 8.2 kcal/mol. See Figure S14 in the Supporting Information.